IEEE Access
Multidisciplinary | Rapid Review | Open Access Journal

Received February 4, 2020, accepted March 18, 2020, date of publication March 23, 2020, date of current version April 6, 2020.

Digital Object Identifier 10.1109/ACCESS.2020.2982581

Distributed Optimal Deployment on a Circle for Cooperative Encirclement of Autonomous Mobile Multi-Agents

PENGPENG YAN[1], YONGHUA FAN[1], RUIFAN LIU[1,2], AND MINGANG WANG[1]
[1]School of Astronautics, Northwestern Polytechnical University, Xi'an 710072, China
[2]Centre for Autonomous and Cyber-Physical Systems, Cranfield University, Bedford MK43 0AL, U.K.

Corresponding author: Yonghua Fan (fyhlixin@163.com)

This work was supported in part by the Aeronautical Science Foundation of China under Grant 20180753007.

ABSTRACT A distributed encirclement points deployment scheme for a group of autonomous mobile agents is addressed in this paper. Herein, each agent can measure its own azimuth related to the common target and can at least communicate with its two adjacent neighbors. Given its space-cooperative character, the encirclement points deployment problem is formulated as the coverage control problem on a circle. The measurement range of azimuth sensor is taken into consideration when doing problem formulation, which is closer to the facts in real-world applications. Then, the fully distributed control protocols are put forward based on geometric principle and the convergence is proved strictly with algebraic method. The proposed control protocols can steer the mobile agents to distribute evenly on the circle such that the coverage cost function is minimized, and meanwhile the mobile agents' spatial order on the circle is preserved throughout the systems' evolution. A noteworthy feature of the proposed control protocols is that only the azimuths of a mobile agent and its two adjacent neighbors are needed to calculate the mobile agent's control input, so that the control protocols can be easily implemented in general. Moreover, an adjustable feedback gain is introduced, and it can be employed to improve the convergence rate effectively. Finally, numerical simulations are carried out to verify the effectiveness of the proposed distributed control protocols.

INDEX TERMS Cooperative encirclement, optimal deployment, autonomous mobile multi-agents, distributed control, uniform coverage control.

I. INTRODUCTION

Recently, cooperative control of autonomous mobile multi-agents has received more and more attention and research due to its widespread applications in the growing variety of team tasks, such as environmental monitoring, transportation, search and rescue, pursuit and evasion [1]–[5]. One typical solution of many-to-one pursuit and evasion problem is cooperative encirclement, where the mobile agents are required to distribute around the target and then enclose it continuously.

According to the above definition, all the following examples [6]–[10] fall into the category of cooperative encirclement control. In [6], the cooperative surrounding control problem for networked multi-agent systems with nonlinear Lagrangian dynamics has been studied; a target-encirclement control protocol of fractional-order multi-agent systems has been presented in [7]; Marshall *et al.* have studied the geometric formations of wheeled vehicles under cyclic pursuit [8]; cooperative hunting task of multi-autonomous underwater vehicle has been studied in [9]; a group of cooperative missiles trying to attack a stationary target from multiple directions has been considered in [10]. On the whole, cooperative encirclement control is a kind of space-cooperative control.

It has been proposed that the cooperative encirclement problem can be decomposed into two independent subproblems: one is to deploy encirclement points and the other is to guide the mobile agents to arrive at their corresponding encirclement points [11]. In accordance with this idea, significant research efforts have been made for the deployment of encirclement points [12]–[16], especially focusing on how to lead the mobile agents distribute evenly on a target-centered circle [11], [17]–[20]. Then, the encirclement points deployment

The associate editor coordinating the review of this manuscript and approving it for publication was Shichao Liu.

problem can be formulated as the coverage control problem on a circle, where the goal is to deploy the mobile agents on the circle so as to satisfy some optimization criteria.

The coverage control methods can be broadly classified into two types: centralized and distributed. Compared to centralized control methods, distributed control methods provide a great implementation advantage and have been paid more attention by scholars. Flocchini *et al.* have studied the self-deployment of mobile sensors on a ring in a purely decentralized and distributed fashion, and they have proved that exact self-deployment is impossible if the sensors do not share a common orientation of the ring [17]. Wang *et al.* have proposed distributed control laws for a group of autonomous mobile agents to realize any given circle formation when the agents move in the one-dimensional space of a circle [11]. Song *et al.* have investigated the coverage problem for mobile sensor networks on a circle while preserving the mobile sensors' spatial order [18]. And the work has been extended in [19] and [20] by taking into consideration mobile sensors' limited communication ranges and input saturation, respectively. From the aforementioned works about distributed coverage control problem on a circle one can know that the mobile agents are usually assumed to be: i) autonomous, i.e., without a central control, ii) anonymous, i.e., indistinguishable from one another, iii) interactive, i.e., can communicate with each other.

There are many kinds of optimization criteria (e.g., to minimize distribution error, to maximize sensing coverage or to minimize the arrival time from the agents to any point on the circle) in the coverage control problem on a circle; see for examples [17]–[20] and the references therein. Minimizing distribution error, which corresponds to uniform coverage, is the essential optimization criterion of coverage control. In many space-cooperative applications such as boundary monitoring and cooperative encirclement mission, the main concern is to deploy the mobile agents such that the circle is covered uniformly. Moreover, the spatial order preservation of the mobile agents is also an important concern because this can avoid collisions between agents throughout the systems' evolution.

The goal of this paper is to design distributed control protocols such that the encirclement points of a group of autonomous mobile agents can reach and remain a state of static equilibrium and distribute evenly on the target-centered circle with order preservation. The mobile multi-agents considered here are autonomous, anonymous, interactive, and randomly dispersed on the given circle. Each agent with onboard navigation sensor can measure its own azimuth, which is an angle between a datum line and the agent-target-line. Note that, the measurement range of navigation sensor is not footloose; in practice, the measured value of azimuth is usually limited in $[-\pi, \pi]$ [21], [22]. This should be considered when doing problem formulation.

The main contributions of this paper can be summarized as follows. Firstly, given its space-cooperative character, the problem of encirclement points deployment is formulated as the problem of coverage control on a circle. Then naturally, the fully distributed control protocols are put forward based on geometric principle and proved strictly with algebraic method. Secondly, the measurement range of azimuth sensor is taken into consideration when doing problem formulation, which is closer to the facts in real-world applications. Thirdly, an adjustable feedback gain is introduced into the proposed distributed control protocols, and it can be employed to improve the convergence rate effectively. Finally, except for encirclement points deployment, the work can also be employed in many other potential applications such as boundary monitoring, collaborative emergency rescue and mobile sensors' uniform coverage.

The remainder of this paper is organized as follows. Preliminaries and problem formulation are presented in Section II. Based on geometric principle of coverage control on a circle, the distributed control protocols are designed in Section III. And Section IV provides the convergence analysis based on algebraic method. In Section V, numerical simulation results are provided to illustrate the effectiveness of the proposed control protocols. Finally, the conclusions of this paper are drawn in Section VI.

II. PRELIMINARIES AND PROBLEM FORMULATION

Consider a group of mobile agents Q_i, $i \in \mathcal{I}_n = \{1, 2, \cdots, n\}$ which are dispersed randomly on the target-centered circle already and no two agents occupy the same position. The position of Q_i can be denoted by its azimuth q_i measured counterclockwise from the common positive horizontal axis Ox to the agent-target-line OQ_i, as shown in Fig.1(a). Without loss of generality, assume that the target-centered circle is a unit circle, then the (x, y) coordinates of Q_i can be expressed as $(\cos q_i, \sin q_i)$.

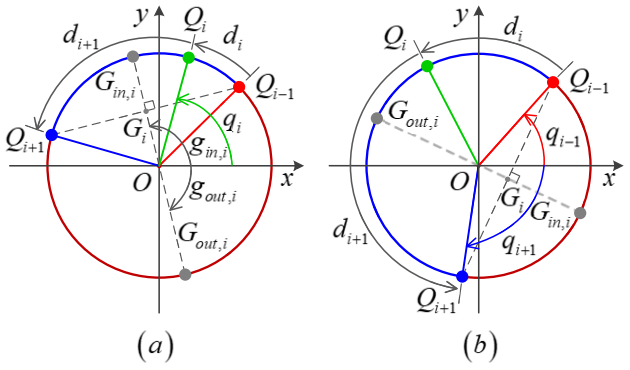

FIGURE 1. Illustration of three neighboring agents distributed on a circle. (a) The case where $0 < d_i + d_{i+1} < \pi$. (b) the other case where $\pi \le d_i + d_{i+1} < 2\pi$. Note that, all the angles in this figure, including $q_i, q_{i-1}, q_{i+1}, g_{in,i}, g_{out,i}$, lie in $[-\pi, \pi]$. The angle's value is positive if an angle's arrow is counterclockwise; the value is negative if an angle's arrow is clockwise.

Given that the measured value of azimuth q_i is limited in $[-\pi, \pi]$ (in radians), the mobile agents can be assumed to

evolve according to the following discrete-time dynamics

$$\begin{cases} q_i'(k+1) = q_i(k) + \tau \cdot u_i(k) \\ q_i(k+1) = \text{atan2}(\sin(q_i'(k+1)), \cos(q_i'(k+1))) \end{cases} \quad (1)$$

where $i = 1, 2, \cdots, n$; $q_i(k)$ represents the Q_i's position at step k; $u_i(k)$ denotes the control input which needs to be designed hereafter; τ is the step-size; the function atan2(y, x) is used to calculate the four-quadrant inverse tangent of the point (x, y) and return a result which lies in $[-\pi, \pi]$ [23], [24].

Remark 1: The atan2(y, x) can be regarded as the polar angle of a complex number $z = x + y$i. It is useful in many applications such as the frequency, phase, and time synchronization of digital communications, digital FM demodulation and the object recognition in image processing [24]. What's more, the function atan2(y, x) is available in many programming languages such as MATLAB. Herein, it's used to deal with the problem that the measured value of azimuth q_i is limited in $[-\pi, \pi]$.

Moreover, the mobile agents are interactive and we assume that each agent can at least communicate with its two adjacent neighbors: left neighbor and right neighbor. The left neighbor of Q_i, which is denoted by Q_{i-1} as shown in Fig.1, is the first mobile agent to be encountered clockwise along the circle. Similarly, Q_i's right neighbor is the first mobile agent to be encountered counterclockwise along the circle, and it's represented by Q_{i+1}.

When no ambiguity arises, we can also say that the left neighbor and right neighbor of q_i are q_{i-1} and q_{i+1}, respectively. In accordance with the initial positions on the circle, we can label the mobile agents counterclockwise as follows

$$-\pi < q_1(0) < q_2(0) < \cdots < q_{n-1}(0) < q_n(0) \leq \pi \quad (2)$$

For the convenience of proof hereafter, let subscript 0 represents n and subscript $n+1$ represents 1 throughout this paper, i.e., $q_0 \equiv q_n$ and $q_{n+1} \equiv q_1$ here. Then q_i's left neighbor is q_{i-1} and q_i's right neighbor is q_{i+1} for $\forall i \in \mathcal{I}_n$. In addition, for our analysis, two definitions are given as follows

Definition 1: The neighboring counterclockwise distance from Q_{i-1} to Q_i, which is denoted by d_i as shown in Fig.1, can be calculated by

$$d_i(k) = q_i(k) - q_{i-1}(k) + \pi \left[1 - \text{sign}(q_i(k) - q_{i-1}(k))\right] \quad (3)$$

where $i = 1, 2, \cdots, n$; sign$(\cdot)$ is the signum function. Given no two agents occupy the same position, one can know that $d_i(k) \in (0, 2\pi)$. Two simple examples are $d_1(0) = q_1(0) - q_n(0) + 2\pi$ and $d_n(0) = q_n(0) - q_{n-1}(0)$.

Definition 2: The error of neighboring counterclockwise distance $e_i(k)$ is defined as follows

$$e_i(k) = d_i(k) - d_{i-1}(k) \quad (4)$$

where $i = 1, 2, \cdots, n$, and especially $e_1(k) = d_1(k) - d_n(k)$. From the range of $d_i(k)$, one has $e_i(k) \in (-2\pi, 2\pi)$.

If $e_i(k) = 0$ holds for $\forall i \in \mathcal{I}_n$, then it's easy to see that $d_1(k) = d_2(k) = \cdots = d_n(k) = 2\pi/n$, which indicates that all mobile agents have distributed evenly on the circle and the uniform coverage has been achieved. Hence, the optimization criteria, namely the coverage cost function, can be introduced as follows

$$T(k) = \sum_{i=1}^{n} |e_i(k)| \geq 0 \quad (5)$$

The smaller the $T(k)$ is, the better the even dispersity of encirclement points will be. In summary, the encirclement points deployment problem can be stated as follows: for a group of autonomous mobile agents subjected to the dynamics (1) and the initial condition (2), the goal of this work is to design distributed control protocols $u_i(k)$ to steer the mobile agents such that the coverage cost function $T(k)$ is minimized, and meanwhile the mobile agents' spatial order on the circle is preserved throughout the systems' evolution.

III. DISTRIBUTED CONTROL PROTOCOLS DESIGN BASED ON GEOMETRIC PRINCIPLE

In this section, we mainly propose the distributed control protocols based on the geometric principle of uniform coverage to minimize the coverage cost function $T(k)$. Before that, two important definitions are given as follows

Definition 3: For an azimuth $q_i(k)$ with a left neighbor $q_{i-1}(k)$ and a right neighbor $q_{i+1}(k)$, its adjacent average-in angle is defined as

$$g_{in,i}(k) = \text{atan2}(\sin q_{i-1}(k) + \sin q_{i+1}(k), \cos q_{i-1}(k) + \cos q_{i+1}(k)) \quad (6)$$

where $g_{in,i}(k) \in [-\pi, \pi]$.

Definition 4: For an azimuth $q_i(k)$ with a left neighbor $q_{i-1}(k)$ and a right neighbor $q_{i+1}(k)$, its adjacent average-out angle is defined as

$$g_{out,i}(k) = \text{atan2}(-\sin q_{i-1}(k) - \sin q_{i+1}(k), -\cos q_{i-1}(k) - \cos q_{i+1}(k)) \quad (7)$$

where $g_{out,i}(k) \in [-\pi, \pi]$.

Subsequently the geometric meanings of adjacent average-in angle $g_{in,i}(k)$ and adjacent average-out angle $g_{out,i}$ are explained according to Fig.1. As mentioned earlier, the (x, y) coordinates of Q_{i-1} and Q_{i+1} can be expressed as $(\cos q_{i-1}(k), \sin q_{i-1}(k))$ and $(\cos q_{i+1}(k), \sin q_{i+1}(k))$, respectively. Hence, the (x, y) coordinates of the midpoint of Q_{i-1} and Q_{i+1}, who is represented by G_i as shown in Fig.1, can be expressed as

$$\frac{1}{2}(\cos q_{i-1}(k) + \cos q_{i+1}(k), \sin q_{i-1}(k) + \sin q_{i+1}(k)) \quad (8)$$

Based on the aforementioned G_i's (x, y) coordinates, one can see that its corresponding four-quadrant inverse tangent is equal to $g_{in,i}(k)$.

The intersection point between the ray OG_i and the unit circle, which is denoted by $G_{in,i}$, is the midpoint of counterclockwise arc $Q_{i-1}Q_{i+1}$. What's more, $G_{in,i}$ and G_i share the identical four-quadrant inverse tangent, namely $g_{in,i}(k)$. Similarly, extend the ray OG_i reversely and it intersects the

circle at $G_{out,i}$. It's easy to see that $G_{out,i}$ is the midpoint of counterclockwise arc $Q_{i+1}Q_{i-1}$ and its corresponding four-quadrant inverse tangent is $g_{out,i}(k)$.

Remark 2: In this paper, a counterclockwise arc Q_aQ_b represents the directed arc from the first point Q_a to the second point Q_b along the circle counterclockwise. And the length of this arc is called counterclockwise distance from Q_a to Q_b.

The counterclockwise distance from Q_{i-1} to Q_{i+1}, which can be expressed as $d_i + d_{i+1}$, has two case in terms of its value: one is $0 < d_i + d_{i+1} < \pi$ as shown in Fig.1(a) and the other is $\pi \leq d_i + d_{i+1} < 2\pi$ as shown in Fig.1(b). In the first case, the midpoint of counterclockwise arc $Q_{i-1}Q_{i+1}$ is $G_{in,i}$, and in the second case, the midpoint of counterclockwise arc $Q_{i-1}Q_{i+1}$ is $G_{out,i}$.

A distributed optimal deployment scheme candidate is that $Q_i, \forall i \in \mathcal{I}_n$ is always steered towards the midpoint of counterclockwise arc $Q_{i-1}Q_{i+1}$. Then according to this idea, the distributed control protocols are proposed as follows

$$u_i(k) = \begin{cases} K \cdot \text{atan2}(\sin(g_{in,i}(k) - q_i(k)), \\ \quad \cos(g_{in,i}(k) - q_i(k))) & \text{if } f_i(k) > 0 \\ K \cdot \text{atan2}(\sin(g_{out,i}(k) - q_i(k)), \\ \quad \cos(g_{out,i}(k) - q_i(k))) & \text{otherwise} \end{cases} \tag{9}$$

where $K > 0$ is an adjustable feedback gain; $f_i(k) = \text{atan2}(\sin(q_{i+1}(k) - q_{i-1}(k)), \cos(q_{i+1}(k) - q_{i-1}(k)))$.

Remark 3: The geometric meaning of $f_i(k)$ can be expounded by the rotation of axes around original point. When the axes in Fig.1 are rotated counterclockwise by $q_{i-1}(k)$, the corresponding rotation matrix is

$$R(q_{i-1}(k)) = \begin{bmatrix} \cos q_{i-1}(k) & \sin q_{i-1}(k) \\ -\sin q_{i-1}(k) & \cos q_{i-1}(k) \end{bmatrix} \tag{10}$$

After the rotation, Q_{i-1} will locate in the new positive axis Ox and Q_{i+1}'s (x, y) coordinates will become

$$R(q_{i-1}(k)) \cdot \begin{bmatrix} \cos q_{i+1}(k) \\ \sin q_{i+1}(k) \end{bmatrix} = \begin{bmatrix} \cos(q_{i+1}(k) - q_{i-1}(k)) \\ \sin(q_{i+1}(k) - q_{i-1}(k)) \end{bmatrix} \tag{11}$$

Obviously, its corresponding four-quadrant inverse tangent is $f_i(k)$. That's to say, $f_i(k)$ is the four-quadrant inverse tangent corresponding to counterclockwise arc $Q_{i-1}Q_{i+1}$. Similarly, the two four-quadrant inverse tangents in (9) correspond to counterclockwise arc $Q_iG_{in,i}$ and counterclockwise arc $Q_iG_{out,i}$, respectively.

Remark 4: Based on the aforementioned analysis, the physical meaning of (9) is clear. Without loss of generality, consider $K = 1$. Now when $f_i(k) > 0$, i.e., $0 < d_i + d_{i+1} < \pi$ as shown in Fig.1(a), $u_i(k)$ is equal to the counterclockwise distance from Q_i to $G_{in,i}$; when $f_i(k) \leq 0$, i.e., $\pi \leq d_i + d_{i+1} < 2\pi$ as shown in Fig.1(b), $u_i(k)$ is equal to the counterclockwise distance from Q_i to $G_{out,i}$. Therefore, $Q_i, \forall i \in \mathcal{I}_n$ is always steered towards the midpoint of counterclockwise arc $Q_{i-1}Q_{i+1}$. Under the proposed distributed control protocols (9), Q_i doesn't cross its left neighbor Q_{i-1} and its right neighbor Q_{i+1} throughout the systems' evolution. Consequently, the mobile agents' spatial order on the circle is always preserved. The convergence and optimality analyses of the proposed distributed control protocols (9) are provided in the next section.

Remark 5: From (6), (7) and (9), one can see that only the azimuths $q_i(k)$, $q_{i-1}(k)$ and $q_{i+1}(k)$ are needed to calculate Q_i's control input $u_i(k)$. That's to say, only the communications between Q_i and its two adjacent neighbors Q_{i-1}, Q_{i+1} are necessary. Hence, the proposed control protocols (9) are fully distributed and can be implemented without knowing the mobile agents' labels.

IV. CONVERGENCE AND OPTIMALITY ANALYSIS BASED ON ALGEBRAIC METHOD

In this section, it is proved that, under the proposed distributed control protocols (9), a group of autonomous mobile agents can finally reach and remain a state of static equilibrium in which they distribute evenly on the circle and the coverage cost function $T(k)$ is minimized. Its strict proof is based on algebraic method mainly.

Lemma 1 [25]: For a row stochastic matrix $\boldsymbol{P} \in \mathbf{R}^{n\times n}$, all its entries are nonnegative and all its row sums are $+1$. If the graph corresponding to $\boldsymbol{P}$ is connected, the $\boldsymbol{P}$ is stochastic, indecomposable and aperiodic (SIA), and there is $\lim_{n\to\infty} \boldsymbol{P}^n = \mathbf{1}_n \boldsymbol{y}^{\mathrm{T}}$, where is $\boldsymbol{y}$ some column vector.

Now, we are ready to present our main result.

Theorem 1: Consider a group of autonomous mobile agents subjected to the dynamics (1), the initial condition (2) and $0 < \tau K < 1$. Under the proposed distributed control protocols (9), the mobile agents will be steered to a static configuration such that the error of neighboring counterclockwise distance $\lim_{k\to\infty} e_i(k) = 0$ holds for $\forall i \in \mathcal{I}_n$.

Proof: Recall *Remark 4* that, when $f_i(k) > 0$, $u_i(k)$ is K times the size of counterclockwise distance from Q_i to $G_{in,i}$ which can be expressed by $K \cdot (d_{i+1}(k) - d_i(k))/2$; when $f_i(k) \leq 0$, $u_i(k)$ is K times the size of counterclockwise distance from Q_i to $G_{out,i}$ which can also be expressed by $K \cdot (d_{i+1}(k) - d_i(k))/2$. Thus, by using $d_i(k)$, $d_{i+1}(k)$, the $u_i(k)$ can expressed in a new and compact form as follows

$$u_i(k) = \frac{K}{2}(d_{i+1}(k) - d_i(k)) \tag{12}$$

Recall *Definition 1* that, $d_i(k)$ is the neighboring counterclockwise distance from Q_{i-1} to Q_i. Therefore, the change of $d_i(k)$ after one step, which can be denoted by $d_i(k+1) - d_i(k)$, is determined by Q_i's azimuth change $\tau \cdot u_i(k)$ and Q_{i-1}'s azimuth change $\tau \cdot u_{i-1}(k)$. Moreover, $d_i(k)$ will increase when Q_i moves along the circle counterclockwise, and $d_i(k)$ will decrease when Q_{i-1} moves along the circle counterclockwise. Thus, one has

$$d_i(k+1) - d_i(k) = \tau \cdot u_i(k) - \tau \cdot u_{i-1}(k) \tag{13}$$

Substituting (12) into (13) yields

$$\begin{aligned} d_i(k+1) &= d_i(k) + \tau \cdot u_i(k) - \tau \cdot u_{i-1}(k) \\ &= d_i(k) + \frac{\tau K}{2}(d_{i+1}(k) - d_i(k)) \end{aligned}$$

$$-\frac{\tau K}{2}(d_i(k)-d_{i-1}(k)) = \frac{\tau K}{2}d_{i-1}(k)+(1-\tau K)d_i(k)+\frac{\tau K}{2}d_{i+1}(k) \quad (14)$$

Then, from (4) and (14) there is

$$\begin{aligned} e_i(k+1) &= d_i(k+1)-d_{i-1}(k+1) \\ &= \frac{\tau K}{2}d_{i-1}(k)+(1-\tau K)d_i(k)+\frac{\tau K}{2}d_{i+1}(k) \\ &\quad -\frac{\tau K}{2}d_{i-2}(k)-(1-\tau K)d_{i-1}(k)-\frac{\tau K}{2}d_i(k) \\ &= \frac{\tau K}{2}(d_{i-1}(k)-d_{i-2}(k))+(1-\tau K)(d_i(k)-d_{i-1}(k)) \\ &\quad +\frac{\tau K}{2}(d_{i+1}(k)-d_i(k)) \\ &= \frac{\tau K}{2}e_{i-1}(k)+(1-\tau K)e_i(k)+\frac{\tau K}{2}e_{i+1}(k) \end{aligned} \quad (15)$$

where $i = 1, 2, \cdots, n$, and as mentioned earlier $e_0(k) \equiv e_n(k)$, $e_{n+1}(k) \equiv e_1(k)$.

The above equations can be rewritten in a highly compact form as follows

$$\boldsymbol{E}(k+1) = \boldsymbol{C}\cdot\boldsymbol{E}(k) \quad (16)$$

where $\boldsymbol{E}(k) = [e_1(k), e_2(k), \ldots, e_n(k)]^{\mathbf{T}}$; the matrix $\boldsymbol{C} \in \mathbf{R}^{n\times n}$ is

$$\boldsymbol{C} = \begin{bmatrix} 1-\tau K & \tau K/2 & 0 & \cdots & \tau K/2 \\ \tau K/2 & 1-\tau K & \tau K/2 & \cdots & 0 \\ \vdots & \vdots & \vdots & \vdots & \vdots \\ 0 & \cdots & \tau K/2 & 1-\tau K & \tau K/2 \\ \tau K/2 & \cdots & 0 & \tau K/2 & 1-\tau K \end{bmatrix} \quad (17)$$

It can be obtained from (16) that

$$\boldsymbol{E}(k) = \boldsymbol{C}^k\cdot\boldsymbol{E}(0) \quad (18)$$

Given $0 < \tau K < 1$ and *Lemma 1*, $\boldsymbol{C}$ is SIA. Thus, one has

$$\lim_{k\to\infty}\boldsymbol{E}(k) = \lim_{k\to\infty}\boldsymbol{C}^k\boldsymbol{E}(0) = \mathbf{1}_{\mathrm{n}}\boldsymbol{w}^{\mathrm{T}}\boldsymbol{E}(0) \quad (19)$$

where $\boldsymbol{w} \in \mathbf{R}^{n\times 1}$ and all its entries are $1/n$.

Considering (4), the following equation holds

$$\begin{aligned} \mathbf{1}_{\mathrm{n}}^{\mathbf{T}}\boldsymbol{E}(0) &= e_1(0)+e_2(0)+e_3(0)+\cdots+e_n(0) \\ &= (d_1(0)-d_n(0))+(d_2(0)-d_1(0)) \\ &\quad +(d_3(0)-d_2(0))+\cdots+(d_n(0)-d_{n-1}(0)) \\ &= 0 \end{aligned} \quad (20)$$

Taking (20) into (19) gives

$$\lim_{k\to\infty}\boldsymbol{E}(k) = \mathbf{1}_{\mathrm{n}}\boldsymbol{w}^{\mathrm{T}}\boldsymbol{E}(0) = \mathbf{0}_{\mathrm{n}} \quad (21)$$

Hence, $\lim_{k\to\infty} e_i(k) = 0$ holds for $\forall i \in \mathcal{I}_n$.

This completes the proof of *Theorem 1*.

Remark 5: From (5) and (21), it's easy to see that $\lim_{k\to\infty} T(k) = 0$, i.e., the coverage cost function $T(k)$ is minimized under the proposed distributed control protocols (9). Moreover, one can know that the convergence is asymptotical. It has been shown in [26] that the convergence rate of (16) is determined by the matrix $\boldsymbol{C}$'s second largest eigenvalue, which can be express as $1-\tau K(1-\cos 2\pi/n)$ [27]. Therefore, for the specific number of agents n and step-size τ, the convergence rate can be improved by increasing the adjustable feedback gain K properly.

Remark 6: The above proof implies that the convergence to uniform coverage relies on the assumptions that each agent can communicate with its two adjacent neighbors and the product τK satisfies $0 < \tau K < 1$. These are convergence conditions for the multi-agent systems subjected to the dynamics (1) under the proposed distributed control protocols (9). It should be noted that the two assumptions are not conservative because the convergence to uniform coverage cannot be realized if either of them is untenable.

Remark 7: From *Theorem 1*, one has $\lim_{k\to\infty} e_{i+1}(k) = 0$. Recalling (4) and (12), there is $\lim_{k\to\infty} e_{i+1}(k) = \lim_{k\to\infty}(d_{i+1}(k)-d_i(k)) = 2/K\cdot\lim_{k\to\infty} u_i(k) = 0$. Hence, $\lim_{k\to\infty} u_i(k) = 0$, i.e., each agent's control input $u_i(k)$ converges to zeros as time goes to infinity. That's to say, the mobile agents are static on the circle when the system evolves into equilibrium state.

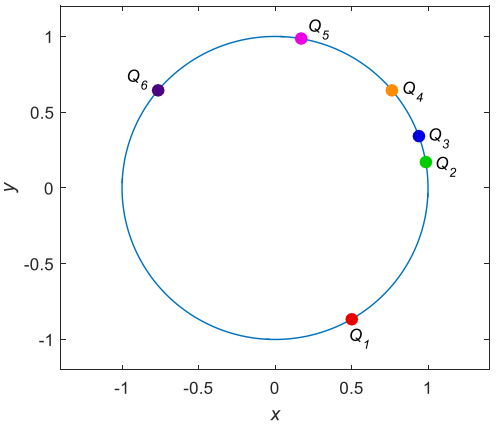

FIGURE 2. A group of six autonomous mobile agents initial positions on the circle.

V. NUMERICAL SIMULATIONS AND ANALYSIS

In this section, some numerical simulations are carried out to verify the effectiveness of the proposed distributed control protocols. Consider a group of six mobile agents which are denoted by colorful solid circles and dispersed randomly on the unit circle already, as shown in Fig.2. Moreover, they can be labeled counterclockwise in accordance with their initial positions on the circle, as mentioned in the inequalities (2). Then, the proposed distributed control protocols (9) are used for realizing the uniform self-deployment of the autonomous mobile agents.

Firstly, a simulation is carried out, in which the step-size τ in (1) and the adjustable feedback gain K in (9) are chosen as 0.1 and 1, respectively. The corresponding simulation results are shown in Figs.3–6. The final deployment positions of

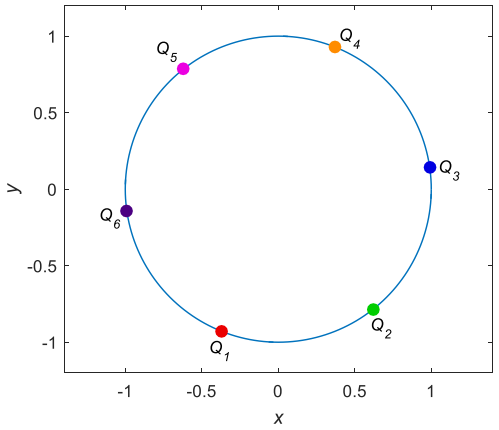

FIGURE 3. Autonomous mobile agents' final deployment positions on the circle.

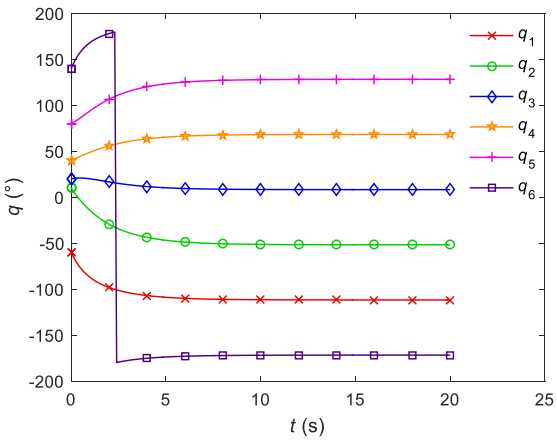

FIGURE 4. Time evolutions of autonomous mobile agents' azimuths. Note that, the agent Q6 passed through the coordinate $(-1, 0)$.

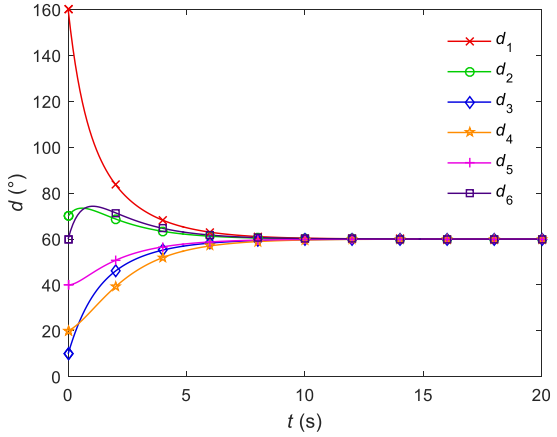

FIGURE 5. Time evolutions of autonomous mobile agents' neighboring counterclockwise distances.

the autonomous mobile agents are illustrated in Fig.3 and it can be seen that the uniform coverage on the circle has been achieved. From Fig.4 one can see that all the azimuths $q_i, i = 1, 2, \cdots, n$ are in keeping with the measurement range of azimuth sensors in real-world scenarios. It can also be seen that the mobile agents' spatial order is preserved

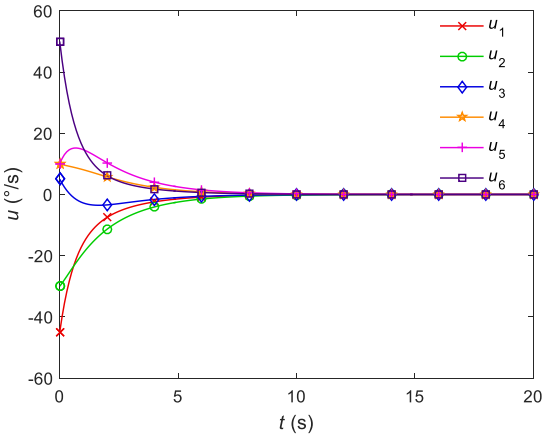

FIGURE 6. Time evolutions of autonomous mobile agents' control inputs.

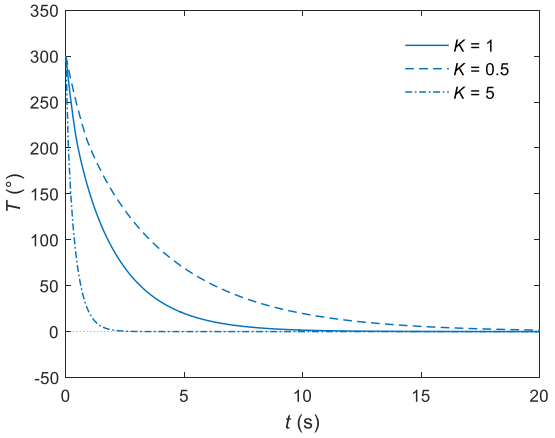

FIGURE 7. Time evolutions of three simulations' coverage cost functions.

throughout the systems' evolution. Moreover, it is noteworthy that Q_6 moves along the circle counterclockwise, passes through the coordinate $(-1, 0)$ and finally stops at its steady-state position. It is clearly shown in Fig.5 that the neighboring counterclockwise distances d_i, $i = 1, 2, \cdots, n$ finally reach consensus and the steady-state values are $(360°/n)|_{n=6} = 60°$. Fig.6 shows the control inputs of the autonomous mobile agents and it is clear that the control inputs u_i, $i = 1, 2, \cdots, n$ eventually converge to zeros, as stated in *Remark 7*.

Furthermore, another two simulations are carried out to illustrate the function of the adjustable feedback gain K. Compared with the first simulation, only the adjustable feedback gains are changed in the two additional simulations, namely $K = 0.5$ and $K = 5$, respectively. Under the proposed control protocols (9), all the mobile agents can reach the identical steady-state positions as shown in Fig.3, although the adjustable feedback gains are different in these three simulations. The time evolutions of the coverage cost functions of the three simulations are shown in Fig.7. It can be seen that all the coverage cost functions are minimized under the proposed control protocols (9), and the convergence rate can be improved by increasing the adjustable feedback gain properly, as mentioned in *Remark 5*.

VI. CONCLUSION

In this study, a distributed encirclement points deployment scheme for a group of autonomous mobile agents has been addressed. Each agent can measure its own azimuth related to the common target and can at least communicate with its two adjacent neighbors. Given its space-cooperative character, encirclement points deployment problem is formulated as the coverage control problem on a circle. Furthermore, the measurement range of azimuth sensor is taken into consideration when doing problem formulation, which is closer to the facts in real-world applications. The proposed control protocols can steer the mobile agents to distribute evenly on the circle such that the coverage cost function is minimized. Meanwhile, the mobile agents' spatial order on the circle is preserved throughout the systems' evolution, which is useful to avoid collisions between agents. A noteworthy feature of the proposed control protocols is that only the azimuths of a mobile agent and its two adjacent neighbors are needed to calculate the mobile agent's control input. It means that the proposed control protocols are fully distributed, which provides a great implementation advantage. Moreover, except for encirclement points deployment, the work can also be employed in many other potential applications such as boundary monitoring, collaborative emergency rescue and mobile sensors' uniform coverage.

Although many advantages and conveniences have been mentioned above, there are still two major limitations in this study that could be addressed in future research. Firstly, the study focused on the uniform deployment on the target-centered circle, and it is incapable of dealing with the nonuniform deployment of heterogeneous autonomous agents. Secondly, under the proposed distributed control protocols, the closed-loop system is asymptotically stable. Note that, in some time-critical applications, convergence time is an important performance index. Although an adjustable feedback gain has been introduced herein and it can improve the convergence rate effectively, the convergence is still asymptotical. Based on the existing results of this study, it is of interest to further study the rapid self-deployment of a group of autonomous mobile agents with pre-given finite convergence time constraint.

REFERENCES

[1] Q. Lu and Q.-L. Han, "Mobile robot networks for environmental monitoring: A cooperative receding horizon temporal logic control approach," *IEEE Trans. Cybern.*, vol. 49, no. 2, pp. 698–711, Feb. 2019.

[2] C. Hu, Z. Zhang, N. Yang, H.-S. Shin, and A. Tsourdos, "Fuzzy multiobjective cooperative surveillance of multiple UAVs based on distributed predictive control for unknown ground moving target in urban environment," *Aerosp. Sci. Technol.*, vol. 84, pp. 329–338, Jan. 2019.

[3] I. H. B. Pizetta, A. S. Brandão, and M. Sarcinelli-Filho, "Avoiding obstacles in cooperative load transportation," *ISA Trans.*, vol. 91, pp. 253–261, Aug. 2019.

[4] F. A. A. Andrade, A. Hovenburg, L. N. D. de Lima, C. D. Rodin, T. A. Johansen, R. Storvold, C. A. M. Correia, and D. B. Haddad, "Autonomous unmanned aerial vehicles in search and rescue missions using real-time cooperative model predictive control," *Sensors*, vol. 19, no. 19, p. 4067, Oct. 2019.

[5] Y. Hou, X. Liang, L. He, and J. Zhang, "Time-coordinated control for unmanned aerial vehicle swarm cooperative attack on ground-moving target," *IEEE Access*, vol. 7, pp. 106931–106940, 2019.

[6] C. Li, L. Chen, Y. Guo, and Y. Lyu, "Cooperative surrounding control with collision avoidance for networked Lagrangian systems," *J. Franklin Inst.*, vol. 355, no. 12, pp. 5182–5202, Aug. 2018.

[7] L. Mo, X. Yuan, and Y. Yu, "Target-encirclement control of fractional-order multi-agent systems with a leader," *Phys. A, Stat. Mech. Appl.*, vol. 509, pp. 479–491, Nov. 2018.

[8] J. A. Marshall, M. E. Broucke, and B. A. Francis, "Formations of vehicles in cyclic pursuit," *IEEE Trans. Autom. Control*, vol. 49, no. 11, pp. 1963–1974, Nov. 2004.

[9] M. Chen and D. Zhu, "A novel cooperative hunting algorithm for inhomogeneous multiple autonomous underwater vehicles," *IEEE Access*, vol. 6, pp. 7818–7828, 2018.

[10] X. Wang, Y. Zhang, and H. Wu, "Distributed cooperative guidance of multiple anti-ship missiles with arbitrary impact angle constraint," *Aerosp. Sci. Technol.*, vol. 46, pp. 299–311, Oct. 2015.

[11] C. Wang, G. Xie, and M. Cao, "Forming circle formations of anonymous mobile agents with order preservation," *IEEE Trans. Autom. Control*, vol. 58, no. 12, pp. 3248–3254, Dec. 2013.

[12] J. Hu and Z. Xu, "Distributed cooperative control for deployment and task allocation of unmanned aerial vehicle networks," *IET Control Theory Appl.*, vol. 7, no. 11, pp. 1574–1582, Jul. 2013.

[13] M. Saska, V. Vonásek, J. Chudoba, J. Thomas, G. Loianno, and V. Kumar, "Swarm distribution and deployment for cooperative surveillance by micro-aerial vehicles," *J. Intell. Robot. Syst.*, vol. 84, nos. 1–4, pp. 469–492, Dec. 2016.

[14] F. Sharifi, A. Chamseddine, H. Mahboubi, Y. Zhang, and A. G. Aghdam, "A distributed deployment strategy for a network of cooperative autonomous vehicles," *IEEE Trans. Control Syst. Technol.*, vol. 23, no. 2, pp. 737–745, Mar. 2015.

[15] G. Franzini and M. Innocenti, "Distributed cooperative deployment of heterogeneous autonomous agents: A Pareto suboptimal approach," *Robotica*, vol. 36, no. 12, pp. 1943–1962, Dec. 2018.

[16] G. Sallam and U. Baroudi, "Cooperative robot deployment: Simulation and real experimental analysis," *Arabian J. Sci. Eng.*, vol. 44, no. 3, pp. 1843–1854, Mar. 2019.

[17] P. Flocchini, G. Prencipe, and N. Santoro, "Self-deployment of mobile sensors on a ring," *Theor. Comput. Sci.*, vol. 402, no. 1, pp. 67–80, Jul. 2008.

[18] C. Song and G. Feng, "Coverage control for mobile sensor networks on a circle," *Unmanned Syst.*, vol. 2, no. 3, pp. 243–248, Jul. 2014.

[19] C. Song and Y. Fan, "Coverage control for mobile sensor networks with limited communication ranges on a circle," *Automatica*, vol. 92, pp. 155–161,Jun. 2018.

[20] C. Song, H. Xu, and Y. Fan, "Circular formation control of mobile agents with limited interaction range and input saturation," in *Proc. IEEE/ASME Int. Conf. Adv. Intell. Mechatronics (AIM)*, Hong Kong, Jul. 2019, pp. 912–917.

[21] H. M. El-Sallabi, W. Zhang, K. Kalliola, and P. Vainikainen, "Full 360° azimuth angle wideband propagation modeling for an urban line-of-sight microcellular environment," in *Proc. IEEE Int. Conf. Commun.*, Vancouver, BC, Canada, vol. 3, Jun. 1999, pp. 1608–1612.

[22] X. Zheng and J. Fu, "Design of magnetic azimuth measurement system based on GMR sensor," in *Proc. 24th Chin. Control Decis. Conf. (CCDC)*, Taiyuan, China, May 2012, pp. 3269–3272.

[23] G. G. Slabaugh, "Computing Euler angles from a rotation matrix," Univ. London, London, U.K., Tech. Rep., Aug. 1999, pp. 39–63.

[24] V. Torres, J. Valls, and R. Lyons, "Fast- and low-complexity atan2(a,b) approximation," *IEEE Signal Process. Mag.*, vol. 34, no. 6, pp. 164–169, Nov. 2017.

[25] W. Ren and R. W. Beard, "Consensus seeking in multiagent systems under dynamically changing interaction topologies," *IEEE Trans. Autom. Control*, vol. 50, no. 5, pp. 655–661, May 2005.

[26] L. Xiao and S. Boyd, "Fast linear iterations for distributed averaging," *Syst. Control Lett.*, vol. 53, no. 1, pp. 65–78, Sep. 2004.

[27] S. Martínez, F. Bullo, J. Cortés, and E. Frazzoli, "On synchronous robotic networks—Part I: Models, tasks, and complexity," *IEEE Trans. Autom. Control*, vol. 52, no. 12, pp. 2199–2213, Dec. 2007.

PENGPENG YAN received the B.S. and M.S. degrees from the School of Astronautics, Northwestern Polytechnical University, Xi'an, China, in 2014 and 2017, respectively, where he is currently pursuing the Ph.D. degree in navigation, guidance, and control. His research interests include flight control, guidance law design, and cooperative control.

YONGHUA FAN received the B.S. degree in mechanics and control from Second Artillery Engineering University, Xi'an, China, in 1998, and the Ph.D. degree in control theory and engineering from Northwestern Polytechnical University, Xi'an, in 2008. He is currently a Professor with the School of Astronautics, Northwestern Polytechnical University. His research interests include guidance and control, advanced control theory, and simulation technique for flight vehicle.

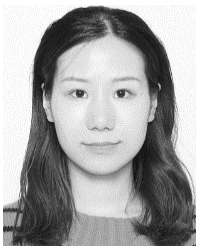

RUIFAN LIU received the B.S. and M.S. degrees from the School of Astronautics, Northwestern Polytechnical University, Xi'an, China, in 2015 and 2018, respectively, where she is currently pursuing the Ph.D. degree in navigation, guidance, and control. She is currently a Visiting Student with the Centre for Autonomous and Cyber-Physical Systems, Cranfield University, U.K. Her research interests include multiple UAV systems, cooperative control, and optimization algorithms.

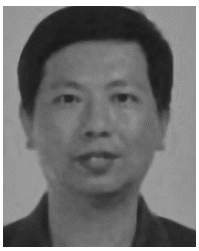

MINGANG WANG was born in 1958. He received the Ph.D. degree from the School of Astronautics, Northwestern Polytechnical University, Xi'an, China. He is currently working as a Professor and the Ph.D. Candidate Supervisor at Northwestern Polytechnical University. His research interests include guidance and control, computer control and simulation, and image processing.